

Systems of vortices in a binary core-shell Bose-Einstein condensate

Victor P. Ruban*

Landau Institute for Theoretical Physics RAS, Chernogolovka, Moscow region, 142432 Russia

(Dated: October 5, 2022)

A trapped Bose-Einstein-condensed mixture of two types of cold atoms with significantly different masses has been simulated numerically within the coupled Gross-Pitaevskii equations. A configuration consisting of a vortex-free core and a shell penetrated by quantum vortices is possible in the phase separation regime. The dynamic properties of vortices in the shell are determined by several parameters. Physically implementable parametric domains corresponding to long-lived strongly nonstationary systems of several vortices attached to the core have been sought. A number of realistic numerical examples of three vortex pairs existing for many hundreds of characteristic times have been presented.

DOI: 10.1134/S0021364022601579

Introduction

In the physics of ultracold Bose-Einstein-condensed gases, a great amount of interest is focused on multicomponent mixtures consisting of different chemical (alkaline) elements, or different isotopes of a single element, or identical isotopes in different (hyperfine) quantum states. These systems in static and dynamic properties are much richer than single-component Bose-Einstein condensates [1–5]. Binary Bose-Einstein condensates are experimentally implemented, for example, in the ^{87}Rb - ^{87}Rb [6], ^{85}Rb - ^{87}Rb [7, 8], ^{39}K - ^{87}Rb [9], ^{41}K - ^{87}Rb [10, 11], ^{23}Na - ^{39}K [12], and ^{23}Na - ^{87}Rb [13] systems.

Sufficiently dilute mixtures of Bose gases with atomic masses m_j in the zero temperature limit can be theoretically studied within the coupled Gross-Pitaevskii equations describing the evolution of the corresponding wavefunctions:

$$i\hbar\partial_t\Psi_j = -\frac{\hbar^2}{2m_j}\nabla^2\Psi_j + \left[V_j(\mathbf{r}) + \sum_k G_{jk}|\Psi_k|^2\right]\Psi_j. \quad (1)$$

Here, $V_j(\mathbf{r})$ is the external potential acting on the j th component of the mixture and G_{jk} is the symmetric matrix of nonlinear interactions given by the expression [2]

$$G_{jk} = 2\pi\hbar^2 a_{jk}(m_j^{-1} + m_k^{-1}), \quad (2)$$

where a_{jk} are the scattering lengths. The Gross-Pitaevskii equations provide the simplest but very comprehensive model of coupled superfluid systems (cf. the review of studies of helium [14]). In particular, since Eq. (1) does not include cross terms in the kinetic energy, the Andreev-Bashkin effect is completely absent; i.e., the superfluid velocity of one component does not contribute to the current of the other component [15, 16].

Some coefficients G_{jk} usually depend on the background uniform magnetic field and can be varied in a

wide desired range using Feshbach resonances [17]. A sufficiently strong cross repulsion between two types of matter waves switches on the spatial separation of phases under the condition [18, 19]

$$G_{12}^2 - G_{11}G_{22} > 0. \quad (3)$$

A relatively narrow domain wall between phases is characterized by the effective surface tension [4, 20]. The spatial separation is mainly responsible for many interesting phenomena such as bubble dynamics [21], quantum analogs of classical hydrodynamic instabilities (Kelvin-Helmholtz [22, 23], Rayleigh-Taylor [24–26], and Plateau-Rayleigh [27]), parametric instability of capillary waves at the interface [28, 29], complex textures in rotating binary condensates [30–32], three-dimensional topological structures [33–37], and capillary flotation of dense droplets in trapped immiscible Bose-Einstein condensates [38].

It is also important that trap potentials are generally different for different types of atoms. For example, the potential of an optical trap formed by laser radiation has the form

$$V_j(\mathbf{r}) = -\frac{\alpha_j}{2}I(\mathbf{r}) + m_jgz, \quad (4)$$

where α_j is the polarizability of an atom of the j th type, $I(\mathbf{r})$ is the time-averaged square of the electric field of laser radiation, and g is the gravitational acceleration. Since the dependence of the polarizability on the frequency of the electromagnetic wave is specific to each component, selecting the frequency of the optical field, one can theoretically control the relative strength of the trap and the spatial positions of minima of the potential for each component [39–41]. It is implied below that either the polarizability ratio is $\alpha_2/\alpha_1 = m_2/m_1$ (at which the gravitational force does not “expand” the minima of the potentials in space), or the system is in free fall state, where it is possible to vary the important parameter

$$\alpha = \alpha_2 m_1 / (\alpha_1 m_2).$$

In this work, the mentioned possible variations of the system parameters are taken into account in the numerical

*Electronic address: ruban@itp.ac.ru

search for optimal regimes for the long-term dynamics of vortex excitations in spherical “core-shell” structures. The ground state of binary Bose–Einstein condensates sometimes has such configurations [42–45]. A core consisting of one component is formed near a sufficiently deep and/or wide minimum of the external potential; the shell of the other component surrounds the core.

Below, we consider the dynamics of several quantized vortex filaments each penetrating the shell toward the core or away from the core (negative or positive vortex, respectively) [46]. An example of the nontrivial dynamics of such attached vortices is shown in Fig. 1 and in video [47]. Similar topological structures in the ^3He – ^4He mixture (a ^4He droplet immersed in liquid ^3He) were qualitatively considered in [48]. The total charge of vortices is always zero. The core remains vortex-free. Two regimes are possible depending on the ratio of the shell thickness to the core size. A more simple (quasi)two-dimensional regime similar to the motion of concentrated vortices in atmospheres of some planets occurs in thin shells. The dynamics in this case is approximately described by the classical model of point vortices on a curved surface [49–51]. The core in this case serves as an almost immobile potential step supporting the shell from inside. The other, three-dimensional, regime is much more complex [46] and occurs when the shell thickness is comparable with the core radius and the core is significantly involved in the dynamics of the system. Depending on the parameters, the effect of the core can be both favorable for the long-term storage of vortices despite their intense interaction and unfavorable.

As recently shown in [46] for the case of equal atomic masses, there is a region of parameters where the undesired process of formation of a close vortex-antivortex pair with the subsequent separation of a vortex filament from the interface with the core is suppressed because of the optimal choice of the coefficients of the nonlinear interaction. In this work, such favorable conditions are determined for the first time in numerous numerical experiments for some mixtures with significantly different atomic masses. It is interesting that configurations where the core consists of lighter atoms and the shell is formed of heavier atoms are optimal for the three-dimensional dynamic regime. In this case, the parameter α equal to the ratio of squares of the eigenfrequencies of the harmonic trap is not unity.

Basic parameters of the model

The quadratic approximation is used for external potentials. Let a harmonic trap be characterized by transverse frequencies $\omega_1 = \omega$ and $\omega_2 = \sqrt{\alpha}\omega$ for atoms of the first type with the mass m_1 forming the shell and for atoms of the second type with the mass m_2 forming the core, respectively. The time, length, and energy will be represented in units of $\tau = 1/\omega$, $l_{\text{tr}} = \sqrt{\hbar/\omega m_1}$, and $\varepsilon = \hbar\omega$, respectively. In real experiments at the

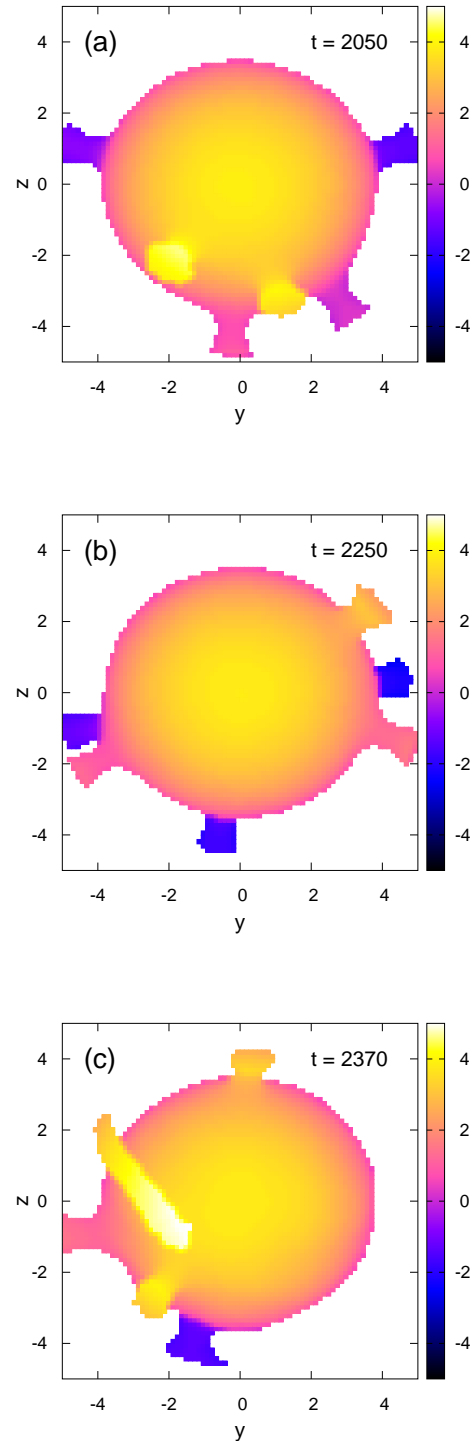


Figure 1: Example of a long-lived nonstationary system of three pairs of attached vortices in the quasi-two-dimensional regime at the compensated gravitational force (i.e., at $\alpha = 1$). The color scale corresponds to the x coordinate of the points of the numerical lattice that are the closest to the surface specified by the equation $|A(\mathbf{r}, t)|^2 = 0.5|A_0(\mathbf{r})|^2$. Only points inside the region $|A_0(\mathbf{r})|^2 > 0.2\mu_1$ are shown; for this reason, the outer ends of vortex filaments are “truncated”.

frequency $\omega/2\pi \sim 100$ Hz, the characteristic length of the trap l_{tr} is about several microns. Since the typical scattering lengths are $a_{jk} \sim a \sim 100a_0$, where a_0 is the Bohr radius, i.e., several nanometers, the inequality $(l_{\text{tr}}/a) \sim 10^3 \gg 1$ necessary for the applicability of the Gross–Pitaevskii equations is certainly satisfied.

The equations of motion for the complex wavefunctions $A(\mathbf{r}, t)$ (shell) and $B(\mathbf{r}, t)$ (core) can be written in the dimensionless form

$$i\dot{A} = -\frac{1}{2}\nabla^2 A + [V + |A|^2 + g_{12}|B|^2] A, \quad (5)$$

$$i\dot{B} = -\frac{1}{2m}\nabla^2 B + [m\alpha V + g_{21}|A|^2 + g_{22}|B|^2] B, \quad (6)$$

where $m = m_2/m_1$ is the ratio of atomic masses, $g_{jk} = G_{jk}/G_{11}$ are the orthonormalized nonlinear coefficients, and $V = (x^2 + y^2 + \lambda^2 z^2)/2$ is the dimensionless potential including the anisotropy parameter λ , taken as $\lambda = 1.1$ to emphasize that the strict spherical symmetry is not necessary.

In this normalization, the conserved numbers of trapped atoms are given by the formulas

$$N_1 = \frac{l_{\text{tr}}}{4\pi a_{11}} \int |A|^2 d^3\mathbf{r} = (l_{\text{tr}}/a_{11})n_1, \quad (7)$$

$$N_2 = \frac{l_{\text{tr}}}{4\pi a_{11}} \int |B|^2 d^3\mathbf{r} = (l_{\text{tr}}/a_{11})n_2. \quad (8)$$

According to these formulas, the realistic numbers $N_1, N_2 \sim 10^6$ correspond to $n_1, n_2 \sim 10^3$.

As known, equilibrium states are characterized by two chemical potentials μ_1 and μ_2 . In our case, $\mu_1 \gg 1$ and $\mu_2 \gg 1$ so that the background profiles of the particle number densities in the shell and core are given in the Thomas–Fermi approximation

$$|A_0|^2 \approx [\mu_1 - V(x, y, z)], \quad (9)$$

$$|B_0|^2 \approx [\mu_2 - m\alpha V(x, y, z)]/g_{22}, \quad (10)$$

respectively. Thus, the effective transverse size of the condensate is $R_{\perp} = \sqrt{2\mu_1}$, whereas the characteristic thickness of vortex filaments in the shell (in the three-dimensional regime) is estimated as $\xi \sim 1/\sqrt{\mu_1}$. Since the chemical potentials in the systems considered below are about several tens (the value $\mu_1 = 18$ was used in numerical experiments), the physical thickness of vortices ξl_{tr} is still larger than the scattering length by orders of magnitude, as should be the case.

In this approximation, the equilibrium shape of the core surface is determined by the requirement of the approximate equality of “hydrodynamic pressures” $P_1 = |A_0|^4/2$ and $P_2 = g_{22}|B_0|^4/2$ (disregarding the surface tension $\sigma \sim |A_0|^3$), i.e.,

$$[\mu_1 - V(x, y, z)] = [\mu_2 - m\alpha V(x, y, z)]/\sqrt{g_{22}}. \quad (11)$$

For the convective stability, the “stratification parameter” should exceed unity:

$$S = m\alpha/\sqrt{g_{22}} > 1. \quad (12)$$

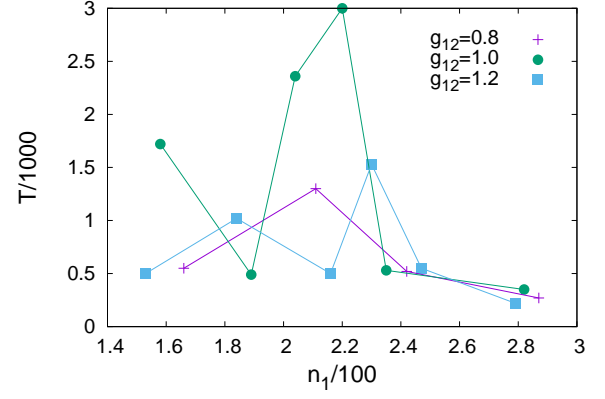


Figure 2: Characteristic lifetime of the system of three pairs of vortices versus the number of atoms of the shell in the ^{23}Na - ^{87}Rb mixture for three g_{12} values. The dependences are irregular because averaging over the initial configurations of vortices was not performed.

At finite μ_1 and μ_2 values, this inequality should be satisfied with some margin because the surface tension against the inhomogeneous background has a destabilizing effect. The optimal S values for the three-dimensional dynamics of attached vortices are in the range of 1.2–1.5, whereas the hard stratification with large S values is better for the quasi-two-dimensional regime.

Numerical results

The equations of motion (5) and (6) were solved numerically by the method described in detail in [46]. The nonlinear coefficients were taken from real data on the scattering lengths for ^{39}K - ^{87}Rb [9], ^{41}K - ^{87}Rb [10, 11], ^{23}Na - ^{39}K [12], and ^{23}Na - ^{87}Rb [13] mixtures.

Three pairs of vortex filaments oriented approximately along three Cartesian axes exist at the initial time. This number of vortices was chosen because the subsequent motion in this case is usually strongly disordered and stimulates the separation of vortex pairs. Since the surface tension confines vortices for a long time in spite of such conditions, this phenomenon is indeed worth studying.

In most simulations, the above separation of the vortex filament from the surface of the core occurred in a certain time after a quite fast dynamics of vortices. Immediately before separation, a vortex-antivortex pair had a V shape, whose base was then separated from the inner boundary of the shell. The time of this event T was fixed as the main result and was used as a rough estimate of the “quality” of the chosen combination of the parameters. Values $T \gtrsim 1000$, which are two orders of magnitude larger than the characteristic period of the trap, can be considered as a good result. In this time, vortices usually many times change their mutual positions,

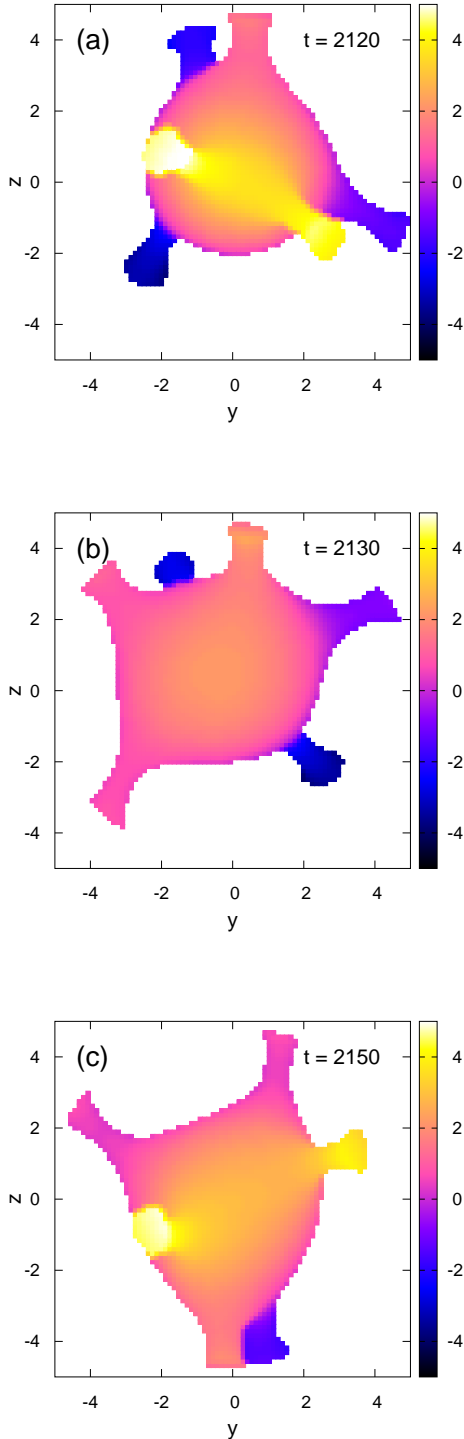


Figure 3: Example of a long-term three-dimensional dynamics of three pairs of attached vortices according to the numerical experiment with the parameters $a_{11} = 88a_0$, $a_{22} = 52a_0$, and $a_{12} = 88a_0$ characteristic of the ^{39}K - ^{23}Na mixture. This gives $m = 0.6$, $g_{22} = 1.0$, and $g_{12} = 1.345$. The number of atoms are $N_1 \approx (l_{\text{tr}}/a_{11}) \times 326$ and $N_2 \approx (l_{\text{tr}}/a_{11}) \times 107$. In contrast to Fig. 1, $\alpha = 2.2$ is used.

constituting long-lived vortex structures. Bose–Einstein condensates in real experiments usually exist in a relatively unchanged form for no more than several seconds. The dimensionless time $T \approx 630$ at the frequency of the trap about 100 Hz corresponds to a real time of 1 s.

Figure 1 shows an example of long-term dynamics in the quasi-two-dimensional regime at the parameters $a_{11} = 52a_0$, $a_{22} = 99a_0$, and $a_{12} = 83a_0$ characteristic of the ^{23}Na - ^{87}Rb mixture [13], which gives $m = 3.78$, $g_{22} = 0.5$, and $g_{12} = 1.0$. The numbers of atoms in this simulation are $N_1 \approx (l_{\text{tr}}/a_{11}) \times 204$ and $N_2 \approx (l_{\text{tr}}/a_{11}) \times 594$. The corresponding video [47] demonstrates a complex behavior of vortices, including the formation of temporal vortex-antivortex pairs, which rapidly move and collide with other vortices. Partners in pairs sometimes change in such collisions. Finally, one of such pairs is separated from the core, as seen in Fig. 1c. The separation of the vortex filament in a thicker shell usually occurs earlier as illustrated in the video in [52]. It is also noteworthy that close vortices with the same sign sometimes form temporal pairs, but they cannot annihilate.

Since not only the number of ^{23}Na atoms in the shell of the ^{23}Na - ^{87}Rb system but also the cross scattering length can be varied, it is of interest to compare the corresponding lifetimes. This comparison is given in Fig. 2. The value $g_{12} = 1.0$ is obviously the most favorable in this case. The lifetime is really a random value because of the chaotic motion of vortices. Consequently, the broken lines in Fig. 2 should be considered only as guides for the eye. The main result seen in this figure is a significant probability of a long lifetime of a complex vortex system.

Qualitatively similar results were obtained for thin shells in the ^{41}K - ^{87}Rb mixture.

Long lifetimes in significantly three-dimensional structures were observed, e.g., for ^{23}Na - ^{39}K mixtures [12], where the lighter element ^{23}Na forms the core and the heavier element ^{39}K constitutes the shell. In this case, the scattering lengths $a_{\text{K-K}}$ and $a_{\text{Na-K}}$ strongly depend on the magnetic field (see Fig. 6 in [12]). A quite large parameter $\alpha = 2.1$ – 2.4 ensures convective stability. The corresponding example is shown in Fig. 3 and in video [53].

The last video [54] concerns the ^{23}Na - ^{87}Rb mixture, where the shell consists of ^{87}Rb atoms. Setting $a_{12} = 99a_0$, we obtain $g_{22} \approx 2.0$ and $g_{12} \approx 2.4$. Since $m \approx 0.26$ in this mixture, sufficiently large α values are necessary for stability. The motion of the vortex configuration with the parameters $\alpha = 7.0$, $n_1 = 333$, and $n_2 = 69$ is relatively regular, as seen in video [54].

Large deviations of the shape of the core from the equilibrium shape are characteristic of three-dimensional dynamics, as in the case of equal atomic masses.

Such expressive results have not yet been obtained for other types of mixtures.

The theoretical consideration with arbitrary dependences of the scattering lengths on the magnetic field and with arbitrary ratios of atomic masses reveals the following approximate symmetry: the three-dimensional

dynamics of two systems with the same α value but with different m values are qualitatively similar (and identically favorable for the storage of vortices) if, first, the stratification parameters are identical,

$$\alpha m^{(1)} / \sqrt{g_{22}^{(1)}} = \alpha m^{(2)} / \sqrt{g_{22}^{(2)}} \approx 1.2 - 1.5,$$

and, second, the surface tension coefficients are equal, which can be ensured by the matching of the cross nonlinear coefficients $g_{12}^{(1,2)}$. Indeed, the hydrodynamic parts of the Lagrangians of both systems can be represented in the same form, and the difference is in “quantum pressures” depending on the masses and in cross nonlinear interactions depending on $g_{12}^{(1,2)}$. However, the role of these terms in long-scale dynamics is reduced only to the surface tension.

This approximate symmetry was confirmed in an example with the parameters $\alpha = 1$, $m^{(1)} = 1$, $g_{22}^{(1)} = 0.6$, $g_{12}^{(1)} = 1.2$ (these values were determined as optimal in [46]) because long-lived attached vortices were also observed in the system with the parameters $m^{(2)} = 2$, $g_{22}^{(2)} = 2.4$, and $g_{12}^{(2)} = 2.4$ – 2.6 .

Conclusions

Thus, numerical examples indicating the possibility of observation of long-term dynamics of bubbles with attached quantum vortices in trapped binary Bose–Einstein condensates with different atomic masses have been demonstrated for the first time. The lifetimes of systems of three pairs of vortices in some numerical experiments are even longer than those in the previously simulated ^{85}Rb – ^{87}Rb mixture with approximately equal masses [46].

It is noteworthy that requirements for the properties of the core are opposite for the quasi-two-dimensional and completely three-dimensional regimes. A hard-trapped, almost immobile heavy core over which the less dense shell easily slips is appropriate for the two-dimensional dynamics of vortices. A light core with an elastic boundary, which is deformed by the tractive force induced by a vortex pair, is appropriate for three-dimensional dynamics. For the same reason, stratification in the three-dimensional case should be not too rigid.

-
- [1] Tin-Lun Ho and V. B. Shenoy, Phys. Rev. Lett. **77**, 3276 (1996).
 - [2] H. Pu and N. P. Bigelow, Phys. Rev. Lett. **80**, 1130 (1998).
 - [3] B. P. Anderson, P. C. Haljan, C. E. Wieman, and E. A. Cornell, Phys. Rev. Lett. **85**, 2857 (2000).
 - [4] S. Coen and M. Haelterman, Phys. Rev. Lett. **87**, 140401 (2001).
 - [5] G. Modugno, M. Modugno, F. Riboli, G. Roati, and M. Inguscio, Phys. Rev. Lett. **89**, 190404 (2002).
 - [6] S. Tojo, Y. Taguchi, Y. Masuyama, T. Hayashi, H. Saito, and T. Hirano, Phys. Rev. A **82**, 033609 (2010).
 - [7] J. P. Burke, Jr., J. L. Bohn, B. D. Esry, and C. H. Greene, Phys. Rev. Lett. **80**, 2097 (1998).
 - [8] S. B. Papp, J. M. Pino, and C. E. Wieman, Phys. Rev. Lett. **101**, 040402 (2008).
 - [9] L. Wacker, N. B. Jørgensen, D. Birkmose, R. Horchani, W. Ertmer, C. Klempt, N. Winter, J. Sherson, and J. J. Arlt, Phys. Rev. A **92**, 053602 (2015).
 - [10] G. Thalhammer, G. Barontini, L. De Sarlo, J. Catani, F. Minardi, and M. Inguscio, Phys. Rev. Lett. **100**, 210402 (2008).
 - [11] A. Burchianti, C. D’Errico, S. Rosi, A. Simoni, M. Modugno, C. Fort, and F. Minardi, Phys. Rev. A **98**, 063616 (2018).
 - [12] T. A. Schulze, T. Hartmann, K. K. Voges, M. W. Gempel, E. Tiemann, A. Zenesini, and S. Ospelkaus, Phys. Rev. A **97**, 023623 (2018).
 - [13] F. Wang, X. Li, D. Xiong, D. Wang, J. Phys. B: At. Mol. Opt. Phys. **49**, 015302 (2016).
 - [14] M. M. Salomaa and G. E. Volovik, Rev. Mod. Phys. **59**, 533 (1987).
 - [15] A. F. Andreev and E. P. Bashkin, Zh. Eksp. Teor. Fiz. **69**, 319 (1975) [JETP **42**, 164 (1976)].
 - [16] G. E. Volovik, Pis’ma v ZhETF **115**, 306 (2022).
 - [17] C. Chin, R. Grimm, P. Julienne, and E. Tiesinga, Rev. Mod. Phys. **82**, 1225 (2010).
 - [18] E. Timmermans, Phys. Rev. Lett. **81**, 5718 (1998).
 - [19] P. Ao and S. T. Chui, Phys. Rev. A **58**, 4836 (1998).
 - [20] B. Van Schaeybroeck, Phys. Rev. A **78**, 023624 (2008).
 - [21] K. Sasaki, N. Suzuki, and H. Saito, Phys. Rev. A **83**, 033602 (2011).
 - [22] H. Takeuchi, N. Suzuki, K. Kasamatsu, H. Saito, and M. Tsubota, Phys. Rev. B **81**, 094517 (2010).
 - [23] N. Suzuki, H. Takeuchi, K. Kasamatsu, M. Tsubota, and H. Saito, Phys. Rev. A **82**, 063604 (2010).
 - [24] K. Sasaki, N. Suzuki, D. Akamatsu, and H. Saito, Phys. Rev. A **80**, 063611 (2009).
 - [25] S. Gautam and D. Angom, Phys. Rev. A **81**, 053616 (2010).
 - [26] T. Kadokura, T. Aioi, K. Sasaki, T. Kishimoto, and H. Saito, Phys. Rev. A **85**, 013602 (2012).
 - [27] K. Sasaki, N. Suzuki, and H. Saito, Phys. Rev. A **83**, 053606 (2011).
 - [28] D. Kobaykov, V. Bychkov, E. Lundh, A. Bezett, and M. Marklund, Phys. Rev. A **86**, 023614 (2012).
 - [29] D. K. Maity, K. Mukherjee, S. I. Mistakidis, S. Das, P. G. Kevrekidis, S. Majumder, and P. Schmelcher, Phys. Rev. A **102**, 033320, (2020).
 - [30] K. Kasamatsu, M. Tsubota, and M. Ueda, Phys. Rev. Lett. **91**, 150406 (2003).
 - [31] K. Kasamatsu and M. Tsubota, Phys. Rev. A **79**, 023606 (2009).
 - [32] P. Mason and A. Aftalion, Phys. Rev. A **84**, 033611 (2011).
 - [33] K. Kasamatsu, M. Tsubota, and M. Ueda, Phys. Rev. Lett. **93**, 250406 (2004).
 - [34] H. Takeuchi, K. Kasamatsu, M. Tsubota, and M. Nitta,

- Phys. Rev. Lett. **109**, 245301 (2012).
- [35] M. Nitta, K. Kasamatsu, M. Tsubota, and H. Takeuchi, Phys. Rev. A **85**, 053639 (2012).
 - [36] K. Kasamatsu, H. Takeuchi, M. Tsubota, and M. Nitta, Phys. Rev. A **88**, 013620 (2013).
 - [37] S. B. Gudnason and M. Nitta, Phys. Rev. D **98**, 125002 (2018).
 - [38] V. P. Ruban, JETP Lett. **113**, 814 (2021).
 - [39] M. S. Safronova, B. Arora, and C. W. Clark, Phys. Rev. A **73**, 022505 (2006).
 - [40] L. J. LeBlanc and J. H. Thywissen, Phys. Rev. A **75**, 053612 (2007).
 - [41] B. Arora, M. S. Safronova, and C. W. Clark, Phys. Rev. A **84**, 043401 (2011).
 - [42] A. A. Svidzinsky and S. T. Chui, Phys. Rev. A **68**, 013612 (2003).
 - [43] S. Gautam and D. Angom, J. Phys. B: At. Mol. Opt. Phys. **43**, 095302 (2010).
 - [44] R. W. Pattinson, T. P. Billam, S. A. Gardiner, D. J. McCarron, H. W. Cho, S. L. Cornish, N. G. Parker, and N. P. Proukakis, Phys. Rev. A **87**, 013625 (2013).
 - [45] A. Wolf, P. Boegel, M. Meister, A. Balaz, N. Gaaloul, and M. A. Efremov, Phys. Rev. A **106**, 013309 (2022).
 - [46] V. P. Ruban, J. Exp. Theor. Phys. **133**, 779 (2021).
 - [47] <http://home.itp.ac.ru/~ruban/28JUL2022/e1.avi>
 - [48] G. E. Volovik, Proc. Natl. Ac. Sci. USA **97**, 2431 (2000).
 - [49] V. P. Ruban, JETP Lett. **105**, 458 (2017).
 - [50] K. Padavić, K. Sun, C. Lannert, and S. Vishveshwara, Phys. Rev. A **102**, 043305 (2020).
 - [51] S. J. Bereta, M. A. Caracanhas, and A. L. Fetter, Phys. Rev. A **103**, 053306 (2021).
 - [52] <http://home.itp.ac.ru/~ruban/28JUL2022/e2.avi>
 - [53] <http://home.itp.ac.ru/~ruban/28JUL2022/e3.avi>
 - [54] <http://home.itp.ac.ru/~ruban/28JUL2022/e4.avi>